

# Directional single-mode emission from coupled whispering gallery resonators realized by using ZnS microbelts

Hai Zhu,<sup>1</sup> Siu Fung Yu,<sup>1,\*</sup> Qi Jie Wang,<sup>2</sup> Chong Xin Shan,<sup>3</sup> and S. C. Su<sup>4</sup>

<sup>1</sup>Department of Applied Physics, The Hong Kong Polytechnic University, Kowloon Hong Kong, China

<sup>2</sup>School of Electrical and Electronic Engineering and School of Physical and Mathematical Sciences, Nanyang Technological University, 639798, Singapore

<sup>3</sup>Changchun Institute of Optics, Fine Mechanics and Physics, Chinese Academy of Sciences, Changchun 130033, China

<sup>4</sup>Institute of Optoelectronic Material and Technology, South China Normal University, Guangzhou 510631, China

\*Corresponding author: sfyu21@hotmail.com

Received January 28, 2013; revised March 12, 2013; accepted March 22, 2013;  
posted March 25, 2013 (Doc. ID 184260); published April 29, 2013

Ring microcavities were formed by wrapping ZnS microbelts, which act as the waveguide and gain region of the microcavities on the surface of optical fibers. The ring microcavities with the formation of whispering gallery modes have lasing threshold lower ( $Q$ -factor higher) than that of the ZnS microbelts. The excitation of TM modes could also be suppressed by the ring geometries of ZnS microbelts. Furthermore, directional single-mode lasing was realized from a coupled asymmetric ring microcavity. The Vernier coupling effect and deformed geometry of the asymmetric ring microcavity were contributed to the stable single-mode operation and directional emission, respectively. © 2013 Optical Society of America

OCIS codes: (140.3410) Laser resonators; (230.4910) Oscillators; (140.7240) UV, EUV, and X-ray lasers.

<http://dx.doi.org/10.1364/OL.38.001527>

Stable and directional single-mode emission can be obtained from semiconductor microcavity lasers with the support of high  $Q$ -factor whispering gallery modes (WGMs) [1]. In order to achieve single-mode operation, it was proposed to use coupled ring microcavities [2] to suppress the excitation of side modes via Vernier coupling effect [3]. Although single-mode emission was observed from CdSe microwires with two coupled micro-loops [4], directional lasing emission was not obtained. In contrast, deformed disk microcavities were proposed to achieve directional lasing emission with high- $Q$  factor WGMs; however, multiple-mode lasing emission was unavoidable [5]. Furthermore, the requirement of using electron-beam lithography and chemical/reactive ion etching to define microcavity lasers on substrates [6] will increase the fabrication complexity and limit the use of semiconductor materials. In this letter, we proposed wrapping semiconductor ZnS microbelts onto the surface of optical fibers to form the building blocks of ring microcavities. By using the advantages of coupled ring microcavities and deformed ring geometries, stable and directional single-mode emission can be achieved.

ZnS microbelts, for which the optical parameters can be found in [7], were grown by a vapor-liquid-solid technique, and the corresponding physical properties are similar to that given in [8]. Ring microcavities were realized by wrapping a ZnS microbelt onto the surface of an optical fiber (with a diameter that varies from 10 to 160  $\mu\text{m}$ ). The two ends of the ZnS microbelt were overlapped each other side-by-side to achieve strong optical coupling. A small amount of silica resin was also applied to the joint in order to fix the microbelt as a ring microcavity. A glass microprobe was used to manipulate the ZnS microbelts. For the fabrication of deformed ring microcavities, two adjacent fibers with different diameters

were glued together by silica resin before the wrap of ZnS microbelts.

Figure 1(a) plots the emission characteristics of a ZnS ring microcavity, which was made by a  $\sim 200$   $\mu\text{m}$  long,  $\sim 5$   $\mu\text{m}$  wide, and  $\sim 200$  nm thick ZnS microbelt on an optical fiber of diameter  $\sim 60$   $\mu\text{m}$ . A quadruplet  $Q$ -switched Nd:YAG laser (at 266 nm) with a pulsed operation ( $\sim 6$  ns, 10 Hz) was used to excite the ring microcavity. The narrowing of spontaneous emission spectrum is observed at the kink of light-light curve. The kink (i.e., pump threshold) is found to be  $\sim 7$   $\text{kW}/\text{cm}^2$ , which is  $\sim 2.3$  times lower than that of the ZnS microbelt Fabry-Perot (FP) cavity even with a length longer than the circumference of the ring microcavity. Mode spacing,  $\Delta\lambda$ , of the ring microcavity is found to be  $\sim 0.27$  nm, which is larger than that of the FP cavity (i.e.,  $\sim 0.14$  nm). Hence, the lasing mechanism of ZnS microbelt has been changed after the formation of ring microcavity.

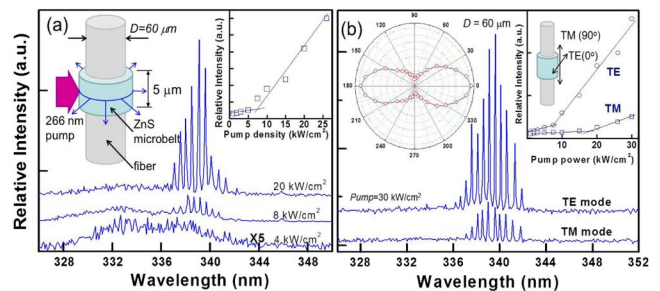


Fig. 1. (a) Lasing spectra of a ring microcavity. Inset on the top-right and top-left corners show light-light curve and schematic diagram of ring microcavity, respectively. (b) Lasing spectra of the two polarizations of the ring microcavity under 30  $\text{kW}/\text{cm}^2$  excitation. Inset on the top-right and top-left corners show the light-light curve and polar plot of the polarization intensity versus rotational angle.

Figure 1(b) shows the polarization characteristics of the ZnS ring microcavity under the pump power of 30 kW/cm<sup>2</sup>. The left inset of Fig. 1(b) displays a polar plot of the lasing modes versus the angle of a linear analyzer. The two light–light curves in Fig. 1(b) were measured by a linear polarizer and a detector. The linear polarization degree,  $\rho$ , of the ZnS microcavity at  $\sim 3$  times the pump threshold is found to be 85%, where  $\rho = (I_{\max} - I_{\min}) / (I_{\max} + I_{\min})$ ;  $I_{\max}$  and  $I_{\min}$  are the maximum and minimum of the output intensity, respectively. This high polarization selection characteristic is due to the geometry of the ring microcavity and the direction of lasing emission. Hence, if the excitation power is below  $\sim 3$  times the pump threshold, the presence of TM modes can be ignored.

The lasing characteristics of ZnS ring microcavities can be investigated by the mode spacing of the ring microcavities,  $\Delta\lambda$ , which is expressed as  $\Delta\lambda = \lambda_o^2 / \pi D n_{\text{eff}}$  where  $\lambda_o$  is the lasing wavelength,  $D$  is diameter, and  $n_{\text{eff}}$  is the effective refractive index. The left inset of Fig. 2 plots the measured values of  $\Delta\lambda$  versus  $1/D$ . By fitting the measured data to the equation with  $\lambda_o$  set to 0.34  $\mu\text{m}$ , it was found that the value of  $n_{\text{eff}}$  is  $\sim 2.2$ . The value of  $n_{\text{eff}}$ , which was also found to be  $\sim 2.27$ , can be estimated by using a simple 1D effective refractive index method [9]. Furthermore, mode spacing ( $\Delta\lambda = \lambda_o^2 / 2Ln_{\text{eff}}$ ) of the microbelt FP cavities is found to be  $\sim 0.13$  nm, where  $L$  ( $\sim 200$   $\mu\text{m}$ ) is the length of the ZnS microbelt. Hence, it is verified that the ring microcavities sustain the formation of WGMs because of the strong optical coupling at the junction. The length of the ZnS microbelt, however, has less influence on the resonant conditions of the ring microcavity, and FP modes are completely suppressed.

Figure 2 also displays the pump threshold and Q-factor ( $\sim \lambda / \delta\lambda$ ) versus  $D$  of the ring microcavities, where  $\delta\lambda$  is the FWHM of lasing peaks. The values of pump threshold and Q-factor for the ZnS microbelt FP cavities with length  $L$ , equal to the circumference of the ring microcavities, are also shown in the figure for comparison. The measured threshold  $P_{\text{th}}$  versus  $D$  of the ring and FP microcavities are also well-fitted by their theoretical formulas,  $P_{\text{th}} \propto \exp(-\alpha D)$  [10] and  $P_{\text{th}} \propto \alpha_i + 2 \ln(1/r) / L$  (i.e., the solid lines), respectively where  $\alpha$ ,  $\alpha_i$ , and  $r$  are constants to be deduced. It is observed that the pump threshold (Q-factor) of the ring microcavities reduces (increases) for  $D > 40$   $\mu\text{m}$  when compared with that of the microbelt FP cavities. This is because the bending loss (i.e., leakage of light from the microcavities resulting

from its curvature) of the ring microcavities is lower than the radiation loss from the facets of the microbelt FP cavities.

The resonant condition of the ring microcavities can be written as  $\pi D n_{\text{eff}} = m\lambda_o$ , where  $m$  is an integer that represents the order of WGMs. The value of  $m$  is determined by the width of the gain spectrum (i.e., between  $\sim 336$  and  $\sim 342$  nm for the ZnS microbelts). To achieve single-mode oscillation, a possible approach is to couple two ring microcavities with different diameters so that the suppression of side modes can be realized by Vernier coupling effect [3]. It is noted that two ring microcavities with diameters  $D$  of  $\sim 45$  and  $\sim 20$   $\mu\text{m}$  will support 6 and 4 WGMs with spacing equal to  $\sim 1.0$  and  $\sim 1.5$  nm, respectively. Hence, if these ring microcavities are optically coupled together, one of the longitudinal modes from both microcavities will only be overlapped within the gain bandwidth. In this case, the longitudinal mode coupled between the two microcavities will then be amplified to achieve single-longitudinal-mode lasing. Figure 3 plots the emission spectra obtained from the individual ring microcavities with  $D = 20$  and 45  $\mu\text{m}$  as well as their coupled two-ring microcavity. The coupled two-ring microcavity was realized by pressing the two microcavities together as shown in the inset of Fig. 3. It is clearly seen that single-mode lasing was supported by the coupled two-ring microcavity at a pump power equal to three times its threshold.

A far-field emission profile of the coupled two-ring microcavity is also shown in the right inset of Fig. 3. It is noted that although the coupled two-ring microcavity supports single-mode lasing, the far-field emission profile is not directional. This is because the strong confinement of WGMs inside the microbelts reduces the constructive interaction of WGMs between the two ring microcavities so that directional emission is difficult to achieve. The measurement was performed by placing a detector 10 cm away from the coupled two-ring microcavity and rotating the detector by  $360^\circ$  in the horizontal plane. A slit of 1 mm wide was also placed in front of the detector.

Directional emission of the ring microcavities can be achieved if a ZnS microbelt is wrapped onto a pair of optical fibers with different diameters. Figures 4(a) and 4(b) show two schematic diagrams of ring microcavities made by two optical fibers of diameters  $D_1$  and  $D_2$ . Measured far-field profiles of the two-ring microcavities are also

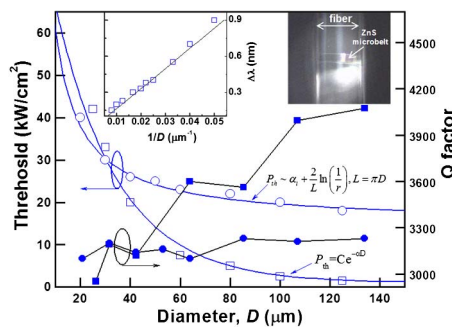


Fig. 2. Plot of threshold “open squares” and Q-factor “filled squares” versus  $D$  of the ring microcavities. The threshold “open circles” and Q-factor “filled circles” of ZnS microbelt FP cavities are also plotted for comparison.

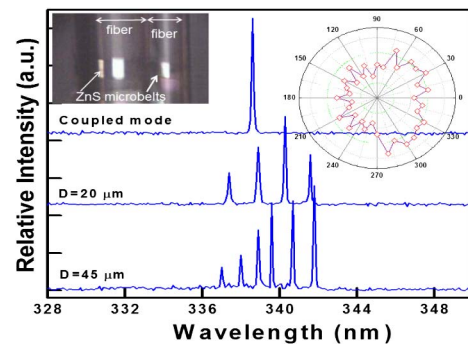


Fig. 3. Measured lasing spectra of the ring microcavities and their coupled two-ring microcavity. Inset on the top-right and top-left corners show far-field profile and photo of the coupled two-ring microcavity, respectively.

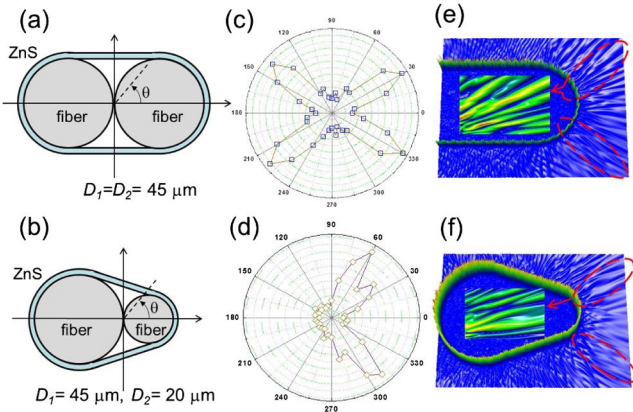


Fig. 4. Schematic diagrams of ring microcavity constructed using two optical fibers with diameters (a)  $D_1 = D_2 = 45 \mu\text{m}$  and (b)  $D_1 = 45 \mu\text{m}$ ,  $D_2 = 20 \mu\text{m}$ . The corresponding measured far-field profiles, and calculated near-field distributions are given in (c), (d) and (e), (f), respectively.

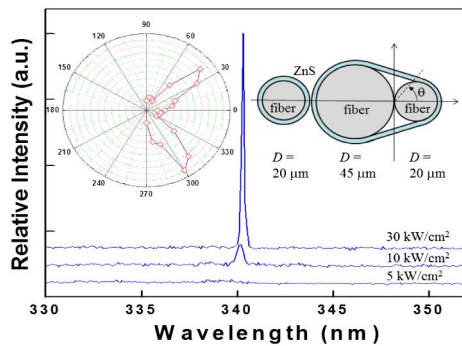


Fig. 5. Lasing spectra of the coupled asymmetric microcavity. Insets on the top-right and top-left corners show the schematic diagram and measured far-field profile of the coupled asymmetric microcavity.

plotted in Figs. 4(c) and 4(d). It is observed that both ring microcavities have a directional emission profile; however, the asymmetric ring microcavity (i.e.,  $D_1 = 45 \mu\text{m}$  and  $D_2 = 20 \mu\text{m}$ ) have better directivity. Figures 4(e) and 4(f) show the calculated near-field emission profile of the ring microcavities using Rsoft FullWAVE. A similar emission profile observed from the experiment can be reproduced through the computer simulation. It is understood that although WGMs are strongly guided inside the ZnS microbelt, radiation is emitted at the region with maximum bending (i.e., highest bending loss). As a result, a directional emission profile can be obtained from the asymmetric ring microcavities. Unfortunately, these ring microcavities support multiple lasing modes.

Single-mode emission can be obtained from the asymmetric ring microcavity, which consists of  $D_1 = 45 \mu\text{m}$  and  $D_2 = 20 \mu\text{m}$ , by optically coupling with another ring microcavity of  $D = 20 \mu\text{m}$ . The inset of Fig. 5 shows the schematic of the proposed coupled asymmetric ring microcavity. Figure 5 plots the lasing emission spectra

of the proposed microcavity laser at a different pump intensity. The pump threshold of the coupled asymmetric ring microcavity is  $\sim 8 \text{ kW/cm}^2$ , which is slightly higher than that of the single-ring microcavity laser ( $\sim 7 \text{ kW/cm}^2$ ) shown in Fig. 1(a). It is recorded that stable single-mode operation can be obtained at high excitation power ( $>$ three times the threshold), and no TM polarization was observed from the emission spectra. The corresponding  $Q$ -factor was found to be  $\sim 3500$ . This value is within the upper limit of measurement. Furthermore, the far-field emission profile of the coupled asymmetric ring microcavity (see the inset of Fig. 5) demonstrates radiation in two directions. Therefore, it is possible to realize directional and stable single-mode emission from the semiconductor microbelts. When compared to the stadium-microcavity lasers (with  $Q$ -factor  $> 10^4$ ) [11], our proposed devices, under the influence of its imperfect curvature at the joint, can still be considered to have a reasonable high value  $Q$  factor.

In conclusion, we have verified that the lasing threshold ( $Q$ -factor) of ZnS microbelts can be reduced (improved) if ring microcavities can be realized from the ZnS microbelts to support WGMs. Directional and stable single-mode emission can also be achieved simultaneously from coupled two-ring microcavities constructed by the ZnS microbelts ring microcavities. In addition, the emission spectra of the coupled two-ring microcavities are mainly dominated by TE polarizations. Hence, it is demonstrated that the ring geometries of ZnS microbelts can be used as the building blocks to fabricate high-optical-quality single-mode single-polarization microcavity lasers.

This work was supported by HK PolyU (Grant Nos. 1-ZV6X, G-YX4P, and G-YJ73). S. C. Su was supported by the National Natural Science Foundation of China (Grant No. 61205037).

## References

1. Z. S. Li, M. Afzelius, J. Zetterberg, and M. Aldén, *Rev. Sci. Instrum.* **75**, 3208 (2004).
2. L. Shang, L. Y. Liu, and L. Xu, *Opt. Lett.* **33**, 1150 (2008).
3. G. Griffel, *IEEE Photon. Technol. Lett.* **12**, 1642 (2000).
4. Y. Xiao, C. Meng, P. Wang, Y. Ye, H. K. Yu, S. S. Wang, F. X. Gu, L. Dai, and L. M. Tong, *Nano Lett.* **11**, 1122 (2011).
5. M. W. Kim, C. H. Yi, S. H. Rim, C. M. Kim, J. H. Kim, and K. R. Oh, *Opt. Express* **13**, 13651 (2012).
6. K. Djordjev, S. J. Choi, P. D. Dapkus, W. Lin, G. Griffel, R. Menna, and J. Connolly, *IEEE Photon. Technol. Lett.* **16**, 828 (2004).
7. J. Valenta, D. Guennani, A. Manar, and B. Hjtnerlage, *Solid State Commun.* **98**, 695 (1996).
8. Y. Wang, L. D. Zhang, C. H. Liang, G. Z. Wang, and X. S. Peng, *Chem. Phys. Lett.* **357**, 314 (2002).
9. <http://wwwhome.math.utwente.nl/~hammer/oms.html>.
10. C. Goyal, R. L. Gallawa, and A. K. Ghatak, *J. Lightwave Technol.* **8**, 768 (1990).
11. H. G. L. Schwefel, H. E. Türeci, A. D. Stone, and R. K. Chang, *Optical Processes in Microcavities* (World Scientific, 2003).